Oxidative addition of Pd to C-H, C-C and C-Cl bonds: Importance of relativistic effects in DFT calculations

Diefenbach, A.; Bickelhaupt, F.M.

published in
Journal of Chemical Physics
2001

DOI (link to publisher)
10.1063/1.1388040

document version
Publisher's PDF, also known as Version of record

Oxidative addition of Pd to C–H, C–C and C–Cl bonds: Importance of relativistic effects in DFT calculations

Axel Diefenbach
Fachbereich Chemie der Philipps-Universität Marburg, Hans-Meerwein-Straße, D-35032 Marburg, Germany

F. Matthias Bickelhaupt[a)]
Afdeling Theoretische Chemie, Scheikundig Laboratorium der Vrije Universiteit, De Boelelaan 1083, NL-1081 HV Amsterdam, The Netherlands

(Received 17 April 2001; accepted 5 June 2001)

To assess the importance of relativistic effects for the quantum chemical description of oxidative addition reactions of palladium to C–H, C–C and C–Cl bonds, we have carried out a systematic study of the corresponding reactions of CH_4, C_2H_6 and CH_3Cl with Pd-d^{10} using nonrelativistic (NR), quasirelativistic (QR), and zeroth-order regularly approximated (ZORA) relativistic density functional theory (DFT) at the BP86/TZ(2)P level. Relativistic effects are important according to both QR and ZORA, the former yielding similar but somewhat more pronounced effects than the latter, more reliable method: activation barriers are reduced by 6–14 kcal/mol and reaction enthalpies become 15–20 kcal/mol more exothermic if one goes from NR to ZORA. This yields, for example, 298 K activation enthalpies $\Delta H^{\neq}_{298}$ of −5.0 (C–H), 9.6 (C–C) and −6.0 kcal/mol (C–Cl) relative to the separate reactants at ZORA-BP86/TZ(2)P. In accordance with gas-phase experiments on reactions of Pd with alkanes, we find reaction profiles with pronounced potential wells for reactant complexes (collisionally stabilized and observed in experiments for alkanes larger than CH_4) at −11.4 (CH_4), −11.6 (C_2H_6) and −15.6 kcal/mol (CH_3Cl) relative to separated reactants [ZORA-BP86/TZ(2)P]. Furthermore, we analyze the height of and the relativistic effects on the activation energies $\Delta E^{\neq}$ in terms of the activation strain $\Delta E^{\neq}_{\text{strain}}$ of and the transition-state interaction $\Delta E^{\neq}_{\text{int}}$ between the reactants in the activated complex, with $\Delta E^{\neq}=\Delta E^{\neq}_{\text{strain}}+\Delta E^{\neq}_{\text{int}}$.
 [DOI: 10.1063/1.1388040]

I. INTRODUCTION

Oxidative addition and reductive elimination [Eq. (1)] are ubiquitous in homogeneous catalysis[1] and have been the subject of many experimental[2–6] and theoretical[7–12] studies:

$$ML_n + R\text{–}X \underset{\text{Reductive Elimination}}{\overset{\text{Oxidative Addition}}{\rightleftharpoons}} R\text{–}ML_n\text{–}X \quad (1)$$

These studies can basically be divided into two groups associated with two different approaches: (i) the experimental or theoretical investigation of particular transition metal complexes (with more or less realistic model systems in the latter case),[1–5,8,9] and (ii) the investigation of the intrinsic reactivity of metal ions or atoms in the absence of ligands or solvent molecules.[4–7,10,11] Experimentally, the latter is realized by mass spectrometric (metal ions)[3–5] and spectroscopic (neutral metal atoms)[6,7] techniques. Theoretical studies[10,11] play a key role in this approach because they allow for an examination of model reactions that are experimentally difficult to realize (or even inaccessible) and yet essential for unraveling a particular problem and achieving profound understanding.

We are interested in the prototypical processes of C–H, C–C and C–Cl bond activation. Whereas in the long term we aim to understand and direct, on the basis of quantum chemical analyses, the factors that determine the catalytic activity of the corresponding transition metal *complexes*, our starting point is the investigation of the *intrinsic* reactivity of the transition metal *atom*. This enables us, in later stages, to precisely assess how ligands alter the metal electronic structure and how they exactly affect the activity and selectivity of the resulting homogeneous catalyst. Thus, recently, we have studied the oxidative addition of Pd-d^{10}+CH_3Cl using nonrelativistic density functional theory (DFT) at the BP86//LDA level.[10] It was shown that the palladium atom has an intrinsic preference for direct oxidative insertion into the C–Cl bond [Eq. (2), OxIn], unlike transition metal complexes such as, e.g., $[Rh(CO)_2I_2]^-$ and $[Rh(CO)_2I_3]^{2-}$ that undergo oxidative addition to CH_3I via an S_N2 pathway.[2p–r] For palladium, this competing nucleophilic substitution mechanism [Eq. (2), S_N2] was found to have an activation energy that is 31 kcal/mol higher than direct oxidative insertion [Eq. (2), OxIn]:

a)Electronic mail: bickel@chem.vu.nl

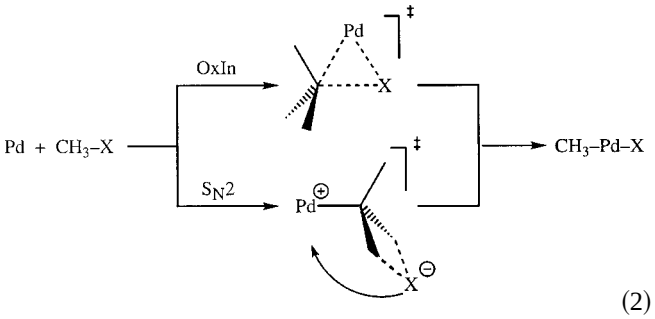

(2)

In the present paper, we extend our previous work in three ways: (i) relativistic effects are incorporated into the theoretical treatment, (ii) the DFT computations are brought to a higher level of theory, and (iii) the set of model substrates is extended to cover the processes of C–H and C–C in addition to C–Cl bond activation, thus describing all three insertion reactions consistently at the same level of theory. The main purpose is to assess the importance of relativistic effects[12] in density functional theoretical (DFT)[13,14] studies on oxidative addition and to provide a sound basis for further theoretical studies on homogeneous catalysis.[15] Thus, we have carried out a systematic investigation on the oxidative insertion of Pd-d^{10} into the C–H, C–C and C–Cl bonds of CH_4, C_2H_6 and CH_3Cl, respectively, using nonrelativistic (NR), quasirelativistic (QR), and zeroth-order regularly approximated (ZORA) relativistic density functional theory (DFT) at the BP86/TZ(2)P level (see Sec. II). The difference in activation energies $\Delta E^{\neq}$ between the different oxidative addition reactions is interpreted and discussed in terms of the activation strain $\Delta E^{\neq}_{\text{strain}}$ of, and the transition-state interaction $\Delta E^{\neq}_{\text{int}}$ between, the reactants in the activated complex, where $\Delta E^{\neq}=\Delta E^{\neq}_{\text{strain}}+\Delta E^{\neq}_{\text{int}}$ (cf. activation strain-TS interaction model[10a]). In particular, we discuss how relativity affects both these barrier heights and the geometries of the corresponding transition states (see Sec. III).

II. METHODS

A. General procedure

All calculations were performed using the Amsterdam Density Functional (ADF) program.[16] The numerical integration was performed using the te Velde scheme.[16b,f,g] The MOs were expanded in a large uncontracted set of Slater type orbitals (STOs) containing diffuse functions: TZ(2)P.[16b,g] The TZ(2)P basis is of triple-ζ quality for all atoms and has been augmented with two sets of polarization functions on maingroup atoms ($3d$ and $4f$ on C and Cl; $2p$ and $3d$ on H) and an extra set of $5p$ functions on palladium. The core shells of carbon ($1s$), chlorine ($1s2s2p$) and palladium ($1s2s2p3s3p3d$) were treated by the frozen-core (FC) approximation.[16b,c] An auxiliary set of *s*, *p*, *d*, *f* and *g* STOs was used to fit the molecular density and to represent the Coulomb and exchange potentials accurately in each SCF cycle.[16b,h]

Energies and geometries were calculated at the nonlocal BP86 level of theory: exchange is described by Slater's $X\alpha$ potential[13a,b] with $\alpha=\frac{2}{3}$ with nonlocal corrections due to Becke[16i,j] and correlation is treated in the Vosko–Wilk–Nusair (VWN, formula *V*) parametrization[16k] with nonlocal corrections due to Perdew[16l] added self-consistently.[16b,m] Equilibrium[16b,n] and transition state[16b,o] structures were fully optimized using analytical gradient techniques. Frequencies[16b,p] were calculated by numerical differentiation of the analytical energy gradients.

Bond enthalpies at 298.15 K and 1 atm (ΔH_{298}) were calculated from 0 K electronic bond energies (ΔE) according to Eq. (3), assuming an ideal gas:[17]

$$\Delta H_{298}=\Delta E+\Delta E_{\text{trans},298}+\Delta E_{\text{rot},298}+\Delta E_{\text{vib},0}+\Delta(\Delta E_{\text{vib}})_{298}+\Delta(pV). \tag{3}$$

Here, $\Delta E_{\text{trans},298}$, $\Delta E_{\text{rot},298}$ and $\Delta E_{\text{vib},0}$ are the differences between products and reactants in translational, rotational and zero point vibrational energy, respectively; $\Delta(\Delta E_{\text{vib}})_{298}$ is the change in the vibrational energy difference as one goes from 0 to 298.15 K. The vibrational energy corrections are based on our frequency calculations. The molar work term $\Delta(pV)$ is $(\Delta n)RT$; $\Delta n=-1$ for two reactants (Pd and CH_3X) combining to one species. Thermal corrections for the electronic energy are neglected.

B. Relativistic effects

Relativistic effects were treated using two different approaches: (i) the quasirelativistic (QR) formalism,[18,19] and (ii) the zeroth-order regular approximation (ZORA).[20]

The quasirelativistic (QR) formalism[18] proceeds from a first-order perturbation approach based on the Pauli Hamiltonian H^{Pauli} [Eq. (4), in atomic units].[19] The latter is obtained from the Dirac Hamiltonian by the procedure of elimination of the small components, followed by an expansion, up to first order, of the resulting operator in $(E-V)/2c^2$ and some manipulations:

$$H^{\text{Pauli}}=V+\frac{p^2}{2}-\frac{p^4}{8c^2}+\frac{\Delta V}{8c^2}+\frac{1}{4c^2}\boldsymbol{\sigma}\cdot(\boldsymbol{\nabla}V\times\mathbf{p}). \tag{4}$$

The first two terms of H^{Pauli} (the potential V and kinetic energy operator $p^2/2$) represent the nonrelativistic Hamiltonian and, in fact, correspond to an expansion up to only zeroth order. The last three terms can be conceived as a first-order relativistic perturbation, consisting of the so-called mass-velocity term $p^4/8c^2$ (a correction to the kinetic energy associated with the relativistic increase of the electron's mass), the Darwin term $\Delta V/8c^2$ (a correction to the effective potential associated with the so-called *Zitterbewegung* of the electron), and the spin-orbit operator (which couples electron spin and orbital momenta). In the present study, only scalar relativistic effects are considered, i.e., the spin-orbit term is not included. In the QR approach, the relativistic energy correction is obtained through diagonalizing the first-order relativistic operator (i.e., the relativistic terms in H^{Pauli}) in the space of zeroth-order solutions (i.e., the nonrelativistic MOs). This turns out to improve results significantly over a simple first-order perturbation treatment. Nevertheless, the QR treatment suffers from a series of problems (see Ref. 20). For example, the expansion used to obtain the Pauli Hamiltonian is invalid for particles in Coulomb potentials because the corresponding (nonrelativistic) eigenstates have compo-

TABLE I. Reaction profiles at BP86/TZ(2)P without and with relativistic effects for the oxidative insertion of Pd into the C–H, C–C, and C–Cl bonds of CH_4, C_2H_6 and CH_3Cl, respectively: 298 K enthalpies (in kcal/mol) relative to reactants, and geometry parameters (in Å, degrees).[a]

	Pd+CH_4 (**1**)			Pd+C_2H_6 (**2**)			Pd+CH_3Cl (**3**)		
	RC	TS	P	RC	TS	P	RC	TS	P
Relative enthalpies									
NR	−6.2	9.2	8.7	−6.1	20.6	5.7	−9.2	−0.4	−20.4
QR	−12.6	−7.6	−13.3	−12.5	7.4	−17.2	−15.5	−7.2	−38.2
ZORA	−11.4	−5.0	−9.7	−11.6	9.6	−14.1	−15.6	−6.0	−35.7
C–X									
NR	1.127	1.712	2.466	1.529	1.997	3.193	1.827	1.969	3.300
QR	1.146	1.484	2.530	1.528	1.879	3.197	1.838	1.919	3.367
ZORA	1.134	1.613	2.412	1.531	1.929	3.002	1.835	1.968	3.169
C–Pd									
NR	2.347	2.067	2.016	3.429	2.118	2.022	3.365	2.364	2.008
QR	2.194	2.055	1.976	3.307	2.085	1.981	3.251	2.573	1.974
ZORA	2.298	2.073	2.000	3.417	2.122	2.001	3.463	2.363	1.987
X–Pd									
NR	1.981	1.558	1.546	2.367	2.118	2.020	2.355	2.433	2.258
QR	1.875	1.552	1.517	2.210	2.085	1.980	2.242	2.314	2.211
ZORA	1.949	1.553	1.527	2.319	2.122	2.001	2.285	2.428	2.227
∠C–Pd–X									
NR	28.6	54.2	86.6	22.3	56.2	102.1	31.4	48.4	101.2
QR	31.5	46.0	91.8	22.7	53.6	107.6	33.1	45.9	107.0
ZORA	29.5	50.3	85.2	21.8	54.1	97.2	29.0	48.5	97.4
Reaction coordinate[b]									
NR	0.02	0.45	1.00	0.00	0.28	1.00	0.01	0.11	1.00
QR	0.04	0.27	1.00	0.00	0.21	1.00	0.02	0.07	1.00
ZORA	0.03	0.39	1.00	0.00	0.27	1.00	0.02	0.12	1.00

[a]NR=nonrelativistic, QR=quasirelativistic, ZORA=zeroth-order regular approximation (Sec. II B). RC=reactant complex, TS=transition state, P=product (Scheme 1 and Fig. 1).

[b]Reaction Coordinate=$[(C–X)-(C–X)_R]/[(C–X)_P-(C–X)_R]$ with (C–X), $(C–X)_R$ and $(C–X)_P$ the C–X bond length in a particular stationary point, in the reactants (i.e., isolated substrate) and in the product, respectively.

nents of high momentum near the nuclei; as a result, the condition $(E-V)/2c^2 \ll 1$ is not satisfied. Another serious problem is that H^{Pauli} is unbound from below which, in principal, implies a core-collapse of the valence MOs. In practice, this collapse is in most, but not all, cases prevented merely by the absence of the highly compact components in the valence basis set that would be necessary for describing the corresponding solutions, i.e., the collapsed MOs.

Most of the problems associated with the Pauli Hamiltonian and the QR approach can be solved[20] if the Hamiltonian resulting from elimination of the small components is expanded in $1/(2c^2-V)$ instead of $(E-V)/2c^2$. To zeroth order, this leads to the ZORA Hamiltonian [Eq. (5), in atomic units].

$$H^{\text{ZORA}} = \boldsymbol{\sigma}\cdot\mathbf{p}\,\frac{c^2}{2c^2-V}\,\boldsymbol{\sigma}\cdot\mathbf{p}+V. \tag{5}$$

In the present study, the performance of the QR and the more reliable ZORA approaches are compared with each other and with the nonrelativistic (NR) DFT results.

C. Analysis of activation barriers

The bonding in transition states for oxidative insertion was analyzed in the conceptual framework provided by the Kohn–Sham molecular orbital (KS-MO) model[14] to gain insight into how the activation barriers of the different oxidative insertion reactions arise and how they are influenced by relativity. This is done using the Activation-strain TS-interaction (ATS) model of chemical reactivity[10a] in which the activation energy $\Delta E^{\neq}$ relative to the separate reactants is decomposed into the activation strain $\Delta E^{\neq}_{\text{strain}}$ and the transition-state (TS) interaction $\Delta E^{\neq}_{\text{int}}$ [Eq. (6)]:

$$\Delta E^{\neq} = \Delta E^{\neq}_{\text{strain}} + \Delta E^{\neq}_{\text{int}}. \tag{6}$$

The activation strain $\Delta E^{\neq}_{\text{strain}}$ is the strain energy associated with deforming the reactants from their equilibrium structure to the geometry they acquire in the activated complex. The TS-interaction $\Delta E^{\neq}_{\text{int}}$ is the actual interaction energy between the deformed reactants in the transition state. In the present study, one of the reactants is the Pd-d^{10} atom and the other reactant is one of the organic substrates CH_4, C_2H_6, and CH_3Cl.

Next, the extended transition state (ETS) method[21] developed by Ziegler and Rauk is used to further decompose the TS interaction $\Delta E^{\neq}_{\text{int}}$ between the strained reactants into three physically meaningful terms [Eq. (7)]:

$$\Delta E^{\neq}_{\text{int}} = \Delta V_{\text{elst}} + \Delta E_{\text{Pauli}} + \Delta E_{\text{oi}}. \tag{7}$$

TABLE II. Reaction profiles obtained with different methods for the oxidative insertion of Pd into the C–H, C–C, and C–Cl bonds of CH_4, C_2H_6 and CH_3Cl, respectively: Zero-Kelvin electronic energies ΔE (in kcal/mol) Relative to reactants (see also Fig. 2) and ZPE-corrected energies $\Delta E + \Delta$ZPE in parentheses.[a]

Reactants	Methods	RC	TS	P	Reference
$Pd+CH_4$ (**1**)	NR-BP86	−5.6(−5.6)	12.6(9.9)	11.3(9.3)	thiswork
	QR-BP86	−11.4(−11.9)	−4.5(−6.9)	−11.0(−12.6)	thiswork
	ZORA-BP86	−10.5(−10.8)	−1.6(−4.2)	−7.1(−9.1)	thiswork
	PCI-80//HF[b]	(−5.1)	(3.6)	(−2.3)	7b
	MCPF//HF[c]	−4	16	9	11j
	CCI+Q//CASSCF[d]	-	15.4	9.1	11l
	CCI+Q//CASSCF[e]	-	25.1	17.6	11l
	GVB-RCI[f]	-	30.5	20.1	11n,o
$Pd+C_2H_6$ (**2**)	NR-BP86	−5.4(−5.7)	23.4(21.1)	8.1(5.6)	thiswork
	QR-BP86	−11.3(−12.0)	10.5(8.2)	−15.0(−17.2)	thiswork
	ZORA-BP86	−10.5(−11.1)	12.5(10.2)	−11.8(−14.1)	thiswork
	PCI-8-//HF[b]	(−6.6)	(19.5)	(−5.5)	7b
	CCI+Q//CASSCF[d]	-	31.5	7.5	11l
	CCI+Q//CASSCF[e]	-	39.2	19.7	11l
	GVB-RCI[f]	-	38.6	16.0	11n,o
$Pd+CH_3Cl$ (**3**)	NR-BP86	−9.5(−9.2)	1.2(0.1)	−19.4(−20.3)	thiswork
	QR-BP86	−15.8(−15.2)	−6.1(−6.7)	−37.2(−38.0)	thiswork
	ZORA-BP86	−15.8(−15.4)	−4.3(−5.6)	−34.8(−35.6)	thiswork
	BP86//LDA[g]	−9.9	1.7	−7.7	10b
	LDA[g]	−23.0	−16.1	−25.3	10b

[a]NR=nonrelativistic, QR=quasirelativistic, ZORA=zeroth-order regular approximation (Sec. II B). RC=reactant complex, TS=transition state, P=product (see Scheme 1 and Fig. 1).
[b]ZPE corrections included. Scalar relativistic effects from first-order perturbation theory.
[c]Scalar relativistic effects from first-order perturbation theory.
[d]Scalar relativistic effects from first-order perturbation theory. CCI+Q refers to multireference externally contracted coupled cluster+Davidson correction.
[e]Same procedure as *d*, except for a smaller basis set.
[f]Relativistic ECPs.
[g]Nonrelativistic and with a smaller basis than in the present work.

The term ΔV_{elst} corresponds to the classical electrostatic interaction between the unperturbed charge distributions of the deformed reactants and is usually attractive. The Pauli-repulsion ΔE_{Pauli} comprises the destabilizing interactions between occupied orbitals and is responsible for the steric repulsion. The orbital interaction ΔE_{oi} accounts for charge transfer (interaction between occupied orbitals on one moiety with unoccupied orbitals of the other, including the HOMO-LUMO interactions) and polarization (empty-occupied orbital mixing on one fragment due to the presence of another fragment).

III. RESULTS AND DISCUSSION

A. Relativistic effects on potential energy surfaces and structures

In this section, we examine the potential energy surfaces (PES) for the various oxidative insertion (OxIn) reactions of $Pd+CH_3X$ using nonrelativistic (NR), quasirelativistic (QR) and ZORA relativistic DFT at the BP86/TZ(2)P level of theory (see Scheme 1, X=H, CH_3, Cl). Our results are summarized in Table I (enthalpies) and II (energies), and in Figs. 1 (reaction profiles) and 2 (geometries).

Each of the three oxidative addition reactions proceeds from the reactants (R) by first forming a reactant complex (RC) which leads, via insertion of the metal atom into the C–X bond, to the transition state (TS) and, finally, the product (P; see Scheme 1 and Fig. 1). The effect of relativity according to both the QR and ZORA approach is that stationary points along the reaction coordinate are stabilized with respect to the reactants, and that this stabilization becomes stronger as the reaction proceeds, i.e., in the order reactant complex (RC)<transition state (TS)<product (P). The effects are slightly less pronounced in ZORA than in QR. This picture emerges from the relative enthalpies in Table I as well as the electronic energies collected in Table II. Note that the relativistic stabilizations of reactant complex and TS are essentially equal in magnitude (ca. 6 kcal/mol) *only* for the insertion of Pd into the C–Cl bond. Let us, for example, take a closer look at the insertion of Pd into the

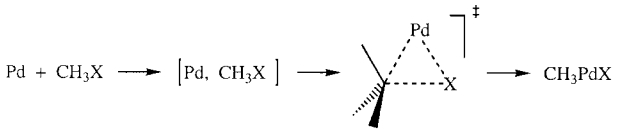

X = H **1a - 1d**
CH_3 **2a - 2d**
Cl **3a - 3d**

Scheme 1. Model Systems and Nomenclature.

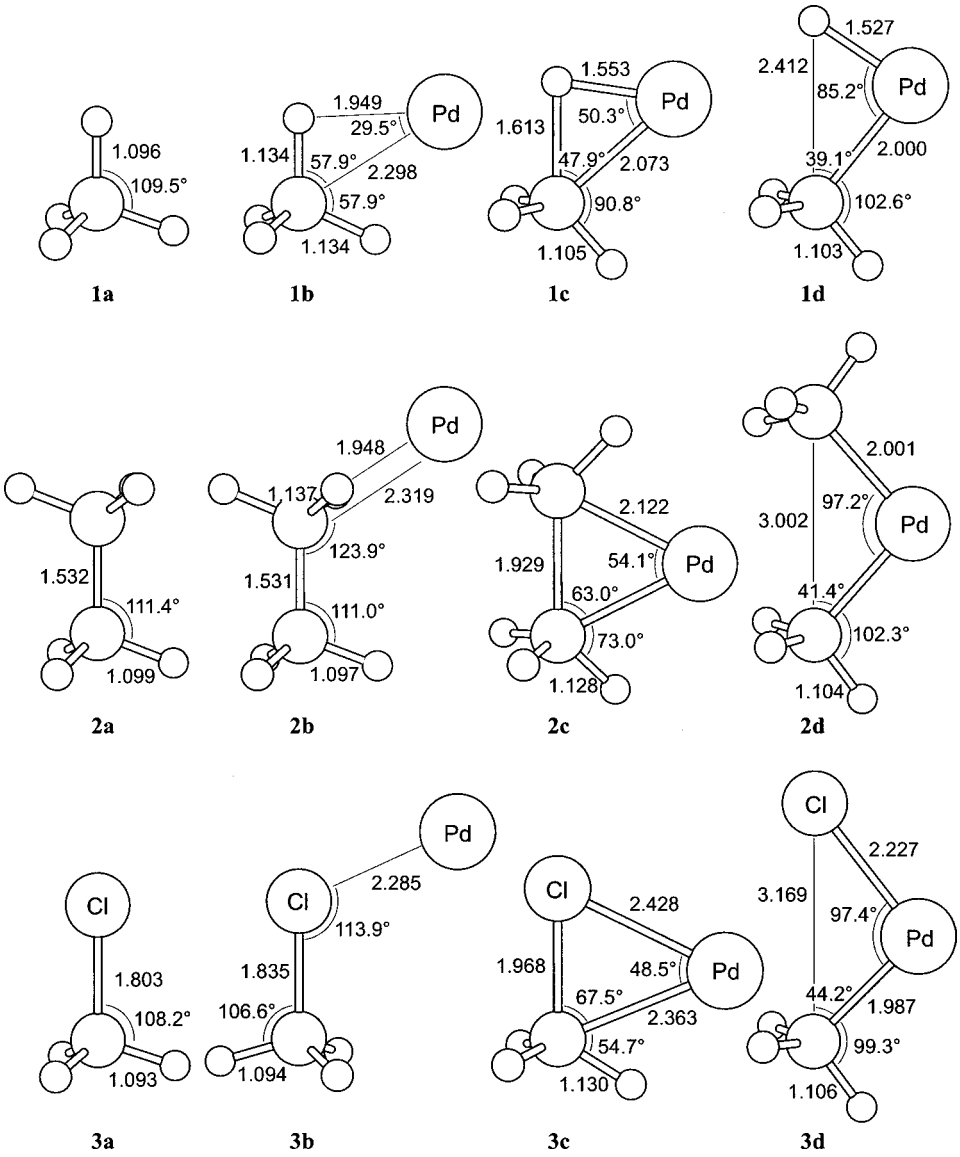

FIG. 1. Geometries (in Å, degrees) of stationary points along the potential energy surface for oxidative insertion (OxIn) of Pd into the C–H, C–C and C–Cl bonds of CH_4 (**1a–1d**), C_2H_6 (**2a**–**2d**) and CH_3Cl (**3a**–**3d**) at ZORA-BP86/TZ(2)P. See also Scheme 1.

C–H bond of methane. The nonrelativistic (NR) relative 298 K enthalpies of the stationary points along the reaction coordinate are 0.0 (R, **1a**), −6.2 (RC, **1b**), 9.2 (TS, **1c**) and 8.7 kcal/mol (P, **1d**; see Table I). The corresponding quasirelativistic (QR) values are 0.0 (**1a**), −12.6 (**1b**), −7.6 (**1c**) and −13.3 kcal/mol (**1d**) and ZORA yields 0.0 (**1a**), −11.4 (**1b**), −5.0 (**1c**) and −9.7 kcal/mol (**1d**). Similar effects can be observed for insertion of palladium into the ethane C–C (**2a**-**2d**) and chloromethane C–Cl bonds (**3a**-**3d**; see Table I). Thus, going from NR to ZORA, activation enthalpies are reduced by 6 (C–Cl) to 14 kcal/mol (C–H) and reaction enthalpies become more exothermic by 15 (C–Cl) to 20 kcal/mol (C–C). This yields 298 K activation enthalpies $\Delta H_{298}^{\neq}$ of −5.0 (C–H), 9.6 (C–C) and −6.0 kcal/mol (C–Cl) relative to the separate reactants at ZORA-BP86. The corresponding reaction enthalpies $\Delta H_{r,298}$ are −9.7 (C–H), −14.1 (C–C) and −35.7 kcal/mol (C–Cl).

The relativistic stabilization of reactant complexes (RC), although weaker than that of transition states and products, is still substantial. This results in pronounced potential wells with complexation enthalpies of −11 kcal/mol for the alkanes (**1b** and **2b**) and −16 kcal/mol for chloromethane (**3b**) at ZORA-BP86. Figure 2 provides a graphical overview of the relativistic effects on potential energy surfaces by comparing the nonrelativistic (left) and ZORA relativistic (right) reaction profiles based on the energies in Table II. Here, it can be clearly seen how relativity significantly reduces the activation barriers for insertion. Note, on the other hand, that the barriers for the reverse reactions, i.e., reductive elimination, become higher. This is of course simply due to the fact that the products (**1d**-**3d**) are more strongly stabilized than the transition states (**1c**-**3c**). Note also that relativistic effects, although sizeable, do not change the relative order of barrier heights and reaction energies or enthalpies (Fig. 2).

How does this compare with the structural effects of relativity? In the first place, the relativistic stabilization of minimum energy structures is accompanied by a shortening of bonds that involve palladium, i.e., C–Pd and X–Pd, as can be seen in Table I for reactant complexes (RC) and products (P). This is in line with general experience.[12b] The relativistic C–Pd and X–Pd bond contractions are somewhat less pronounced for ZORA than for QR. We take again the reac-

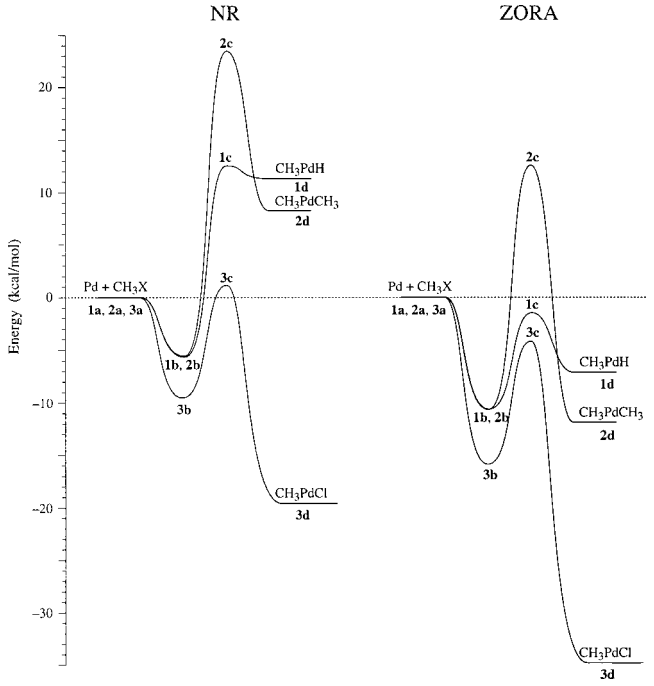

FIG. 2. Relative zero-Kelvin electronic energies (in kcal/mol) of stationary points along the potential energy surface for oxidative insertion (OxIn) of Pd into the C–H, C–C and C–Cl bonds of CH_4 (**1**), C_2H_6 (**2**) and CH_3Cl (**3**) at nonrelativistic (NR, left) and ZORA relativistic (right) BP86/TZ(2)P (see Table II). See also Scheme 1.

tion of $Pd+CH_4$ as an example. In the reactant complex **1b**, Pd has short contacts to both C and X (=H). If we go from NR to ZORA, the C–Pd bond length decreases from 2.347 to 2.298 Å in the reactant complex (**1b**) and from 2.016 to 2.000 Å in the product **1d**. Likewise, the H–Pd bond shrinks from 1.981 to 1.949 Å in **1b** and from 1.546 to 1.527 Å in **1d**. Similar effects occur for insertion of palladium into the ethane C–C (**2b** and **2d**) and chloromethane C–Cl bonds (**3b** and **3d**; see Table I). Note that the metal-substrate interaction in the reactant complexes **2b** and **3b** differs from that in **1b** (see Fig. 1 and Table I). In **2b**, Pd binds to ethane via two C–H bonds of a methyl group instead of forming direct C–Pd and X–Pd bonds (X=C). In **3b**, Pd binds to the substrate predominantly via X (=Cl) and not via C. Thus, the primary effect of relativity is Cl–Pd contraction while there is no pronounced trend for the C–Pd distance. In fact, the latter contracts for QR (from 3.365 to 3.251 Å) and expands for ZORA (from 3.365 to 3.463 Å; see Table I).

Another striking effect is the relativistic *contraction* of the activated C–X bond in the transition states (see Table I). It is strongest for the TS of C–H insertion (**1c**) and becomes less pronounced for the transition states of C–C (**2c**) and C–Cl (**3c**) insertion. For example, going from NR to ZORA, the C–X distance decreases by 0.1 Å in **1c** (from 1.712 to 1.613 Å), by 0.07 Å in **2c** (from 1.997 to 1.929 Å) and by only 0.001 Å in **3c** (from 1.969 to 1.968 Å). To enable a more straightforward comparison of the effect in the different reactions, we define a reaction coordinate R based on the C–X bond length [Eq. (8)]:

$$R=[(C-X)-(C-X)_R]/[(C-X)_P-(C-X)_R]. \quad (8)$$

Here, (C–X) is the C–X bond length in a particular stationary point and $(C-X)_R$ and $(C-X)_P$ are the C–X bond length in the reactants (i.e., isolated substrate) and in the product, respectively. Thus, R=0 at the beginning of the reaction

TABLE III. Analysis of the activation energies for the oxidative insertion reaction of Pd with CH_4, C_2H_6 and CH_3Cl, without and with relativistic effects, in terms of the activation strain model.[a]

		Pd+CH_4 (**1**)			Pd+C_2H_6 (**2**)			Pd+CH_3Cl (**3**)		
		NR	QR	ZORA	NR	QR	ZORA	NR	QR	ZORA
Activation energy analysis (kcal/mol)										
ΔV_{elst}		−177.4	−166.1	−170.4	−139.7	−153.6	−139.5	−74.5	−81.2	−76.7
ΔE_{Pauli}		220.7	213.3	211.1	196.4	218.1	192.6	110.9	114.5	112.3
ΔE_{oi}		−93.5	−90.9	−95.8	−76.4	−87.2	−79.9	−43.7	−42.8	−48.7
$\Delta E^{\neq}_{int}$		−50.2	−43.7	−55.1	−19.7	−22.7	−26.8	−7.3	−9.5	−13.1
$\Delta E^{\neq}_{strain}$		62.8	39.2	53.5	43.1	33.2	39.3	8.5	3.4	8.8
$\Delta E^{\neq}$		12.6	−4.5	−1.6	23.4	10.5	12.5	1.2	−6.1	−4.3
Fragment orbital overlaps ⟨Pd| substrate⟩										
⟨4*d*|LUMO⟩		0.331	0.297	0.327	0.134	0.131	0.129	0.086	0.044	0.082
⟨5*s*|HOMO⟩		0.400	0.368	0.401	0.197	0.185	0.213	0.136	0.148	0.144
Fragment orbital populations (electrons)										
Pd:	4*d*	9.34	9.33	9.32	9.54	9.36	9.42	9.60	9.61	9.59
	5*s*	0.27	0.35	0.38	0.09	0.17	0.22	0.11	0.25	0.18
Substrate:	HOMO	1.76	1.75	1.71	1.88	1.87	1.83	1.94	1.93	1.91
	LUMO	0.39	0.27	0.36	0.27	0.22	0.25	0.16	0.09	0.17
Fragment orbital energies (eV)										
Pd:	4*d*	−4.241	−4.186	−4.193	−4.241	−4.186	−4.193	−4.241	−4.186	−4.193
	5*s*	−2.941	−3.504	−3.423	−2.941	−3.504	−3.423	−2.941	−3.504	−3.423
Substrate:	HOMO	−7.234	−7.685	−7.435	−7.114	−7.532	−7.142	−7.107	−7.073	−7.303
	LUMO	−2.111	−0.878	−1.625	−0.713	−0.041	−0.306	−2.052	−1.538	−2.066

[a]At BP86/TZ(2)P. See Sec. II C. NR=nonrelativistic, QR=quasirelativistic, ZORA=zeroth-order regular approximation (Sec. II B). All analyses have been carried out using the same method for relativistic effects as in the geometry optimization.

(i.e., for the reactants) and R=1 when the reaction has been completed (i.e., for the products). As can be seen in Table I (e.g., for ZORA-BP86), the extent of C–X bond elongation in the TS is highest for the most endothermic reaction, that is, insertion of Pd into the C–H bond (**1c**: R=0.45), and lowest for the most exothermic reaction, that is, insertion of Pd into the C–Cl bond (**3c**: R=0.12). This fits in nicely with the Hammond postulate[22] for transition states of homologous reaction systems (compare Table I and Fig. 2). Note that the relativistic *contraction* of the C–X bond in the TS corresponds to a shift in character of the latter toward the educt. Note also that this occurs together with a relativistic increase in the reaction exothermicity. This is again reminiscent of the Hammond postulate. We return to this point in Sec. III C.

In conclusion, in our BP86/TZ(2)P calculations on the insertion of Pd into C–X bonds, relativity leads to more pronounced potential wells for the reactant complexes, lower activation barriers and more eductlike transition states, as well as more exothermic overall reaction enthalpies.

B. Comparison with experiments and other computations

In this section, we compare our results with those of previous experimental and theoretical investigations. Our findings are consistent with gas-phase experiments of Weisshaar and co-workers[6e,f,7b,e] who studied the reactions of neutral transition metal atoms with alkanes in He buffer gas using spectroscopic techniques. They found that Pd-d^{10} atoms insert neither into the C–H nor the C–C bonds of methane and ethane. No reaction at all is observed for $Pd+CH_4$ whereas $Pd+C_2H_6$ leads to the formation of a collisionally stabilized $[Pd, C_2H_6]$ complex with an effective bimolecular rate constant of $0.16(2)\cdot 10^{-12}\,cm^3\,molecule^{-1}\,s^{-1}$ (refined value from Ref. 7b).[6f,7b,e] The exponential decay of the Pd signal versus alkane pressure furthermore suggested a complexation energy of at least 8 kcal/mol for Pd-alkane complexes.[6f] This lower bound agrees well with our relativistic complexation energies (Table II, ZORA: −10.5 kcal/mol, QR: −11.4 and −11.3 kcal/mol for CH_4 and C_2H_6). On the other hand, our nonrelativistic (NR: −5.6 and −5.4 kcal/mol), but also the PCI-80 complexation energies of Carroll *et al.*[7b] (−5.1 and −6.6 kcal/mol), are slightly too weak compared to experiment. The absence of a complex of Pd and methane in the experiments has been ascribed to a lifetime of the internally hot $[Pd, CH_4]^*$ encounter complex that is too short to allow for collisional cooling.[6f] The larger alkanes, starting with ethane, have more internal degrees of freedom and they more efficiently dissipate the internal energy. Thus, lifetimes of the [Pd,alkane]* encounter complex become long enough to benefit from termolecular cooling.

The fact that no products of C–H or C–C oxidative addition are observed can be understood if both the energy barrier and the entropy or statistical bottleneck are taken into account. In the case of $Pd+CH_4$, the internally hot $[Pd, CH_4]^*$ encounter complex dissociates back to the separate reactants rather than proceeding via the TS for C–H insertion, even though the latter has essentially the same energy as the former ($\Delta E^{\neq}=-1.6$ kcal/mol at ZORA-BP86 and 3.6 kcal/mol at PCI-80, see Table II). This can be ascribed to the high density of states of the unbound reactants and the low density of states of the tight TS for insertion as suggested by the negative activation entropy $\Delta S^{\neq}$ of −22.5 cal/mol K relative to reactants (298 K; at ZORA-BP86; not shown in the tables). Such statistical barriers are well-known and often play a key role in gas-phase ion-molecule reactions.[23] In the case of $Pd+C_2H_6$, insertion into the C–C bond is prevented by an even less favorable entropy bottleneck associated with a negative activation entropy of −26.1 cal/mol K relative to reactants (298 K; at ZORA-BP86; not shown in the tables) and, in addition, a rather high activation energy of 12.5 kcal/mol at ZORA-BP86 (Table II).

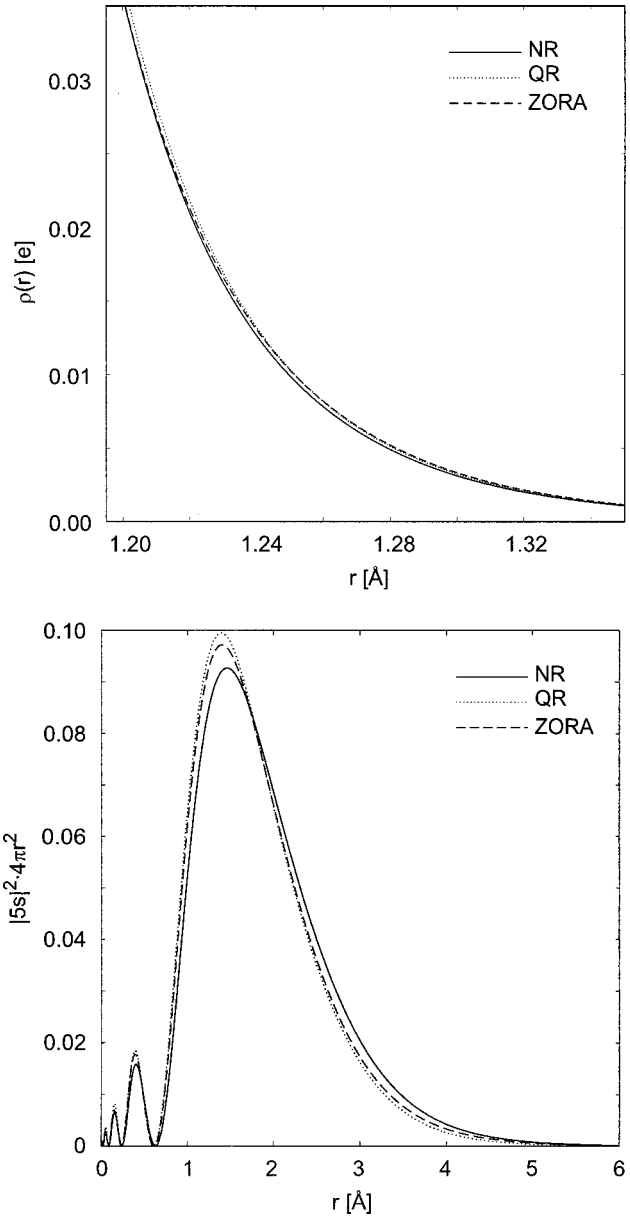

FIG. 3. Radial distribution function of the Pd 5s AO (left) and the electron density of Pd (right) at nonrelativistic (NR), quasirelativistic (QR) and ZORA relativistic BP86/TZ(2)P.

Blomberg, Siegbahn and co-workers[7b,11b,j] have studied the oxidative addition of Pd (and other metal atoms) into the C–H and C–C bonds of methane and ethane (but not chlo-

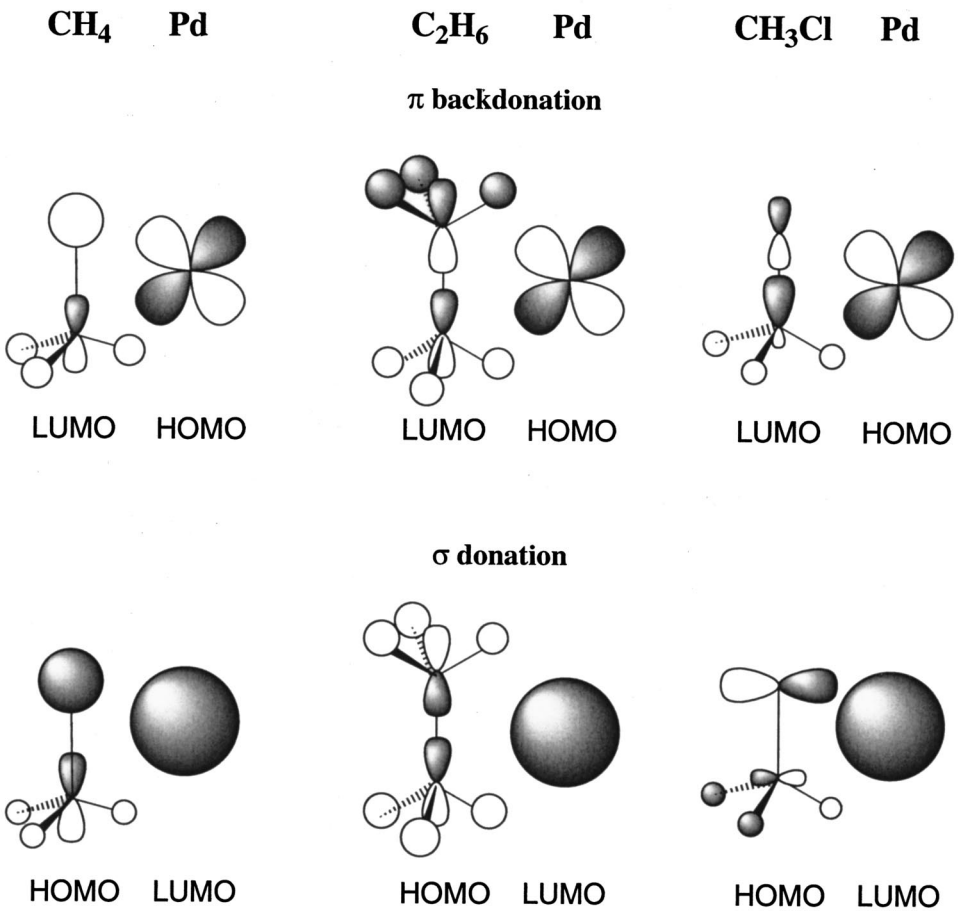

FIG. 4. Schematic representation of the frontier orbital interactions between Pd and the substrate in the transition states for oxidative insertion into the C–H, C–C and C–Cl bonds of CH_4, C_2H_6 and CH_3Cl, emerging from our Kohn–Sham MO analysis of the TS interactions $\Delta E_{\text{int}}^{\neq}$ at nonrelativistic (NR), quasirelativistic (QR) as well as ZORA relativistic BP86/TZ(2)P.

romethane) at PCI-80 in which relativistic effects are accounted for by first-order perturbation theory. With an estimated accuracy of some 3 kcal/mol,[7b] PCI-80 may be considered the best *ab initio* benchmark at present. In the first place, we note a remarkably strong dependence of the computed kinetic and thermodynamic parameters on the level of theory. For example, since the early GVB-RCI calculations of Low and Goddard,[11n,o] the value for the activation energy of Pd insertion into the methane C–H bond has decreased from 30.5 (no ZPE correction) to 3.6 kcal/mol (ZPE-corrected) at PCI-80, i.e., by approximately 27 (!)kcal/mol. Even the more recent MCPF value of 16 kcal/mol (no ZPE correction)[11j] is still some 12 kcal/mol above the PCI-80 barrier of 3.6 kcal/mol (ZPE-corrected). Now, the qualitative trends for potential energy surfaces of $Pd+CH_4$ and $Pd+C_2H_6$ are similar for our NR-, QR-, and ZORA-BP86 as well as the PCI-80 computations (Table II): C–H insertion has a lower barrier and is (slightly) more exothermic than C–C insertion. The best overall agreement of our relativistic BP86/T2(2)P results with PCI-80 is achieved using the ZORA approach. Our ZPE-corrected ZORA-BP86 activation energies are 8–9 kcal/mol below the PCI-80 values, in line with the general tendency of present-day gradient-corrected DFT to underestimate reaction barriers.[13c] The absence of relativistic corrections in the NR-BP86 approach masks this deficiency and yields instead activation energies that are 2–6 kcal/mol *higher* than those of PCI-80. We wish to point out that the PCI-80 activation barriers were computed using two approximations: (i) the final scaled MCPF energies of the PCI-80 study were not computed at the MCPF but instead the HF optimum geometry;[7b,11a] (ii) the TS optimization[11a,j] for $Pd+CH_4$ was carried using the C–Pd and H–Pd distances obtained by Low and Goddard[11n] at HF. This may also contribute to the discrepancies with our ZORA-BP86 results. Furthermore, our ZPE corrected reaction energies at ZORA-BP86 are 7–9 kcal/mol more exothermic than those obtained at PCI-80. Finally, we wish to emphasize that whereas the quasirelativistic approach to relativity is known to fail in a few cases due to the core-collapse mentioned in Sec. II B, such a complete failure apparently does not occur here. Deviations between QR-BP86 and PCI-80 relative energies are only 1–4 kcal/mol larger than those between ZORA-BP86 and PCI-80.

Previously, Bickelhaupt *et al.*[10b] studied the insertion of Pd into the chloromethane C–Cl bond at the BP86//LDA level of DFT without relativistic corrections. As can be seen in Table II, the older BP86//LDA relative energies agree well with those of the present nonrelativistic NR-BP86 computations for the reactant complex (RC, **3b**) and the transition state (TS, **3c**) but they differ significantly for the product (P, **3d**) which is at too high energy in case of BP86//LDA. The discrepancy is caused by the use in the latter[10b] of a smaller basis set (DZP instead of TZ2P for C and H) and LDA instead of BP86 for geometry optimization.

In conclusion, we achieve the best overall agreement with PCI-80 benchmark values using the ZORA-BP86 ap-

TABLE IV. Analysis of the Pd–CH_4 interaction in the transition state for oxidative insertion (**1c**), without and with relativistic effects.[a]

	NR//NR	QR//NR	ZORA//NR
Activation energy analysis (in kcal/mol)			
ΔV_{elst}	−177.4	−179.7	−179.2
ΔE_{Pauli}	220.7	216.1	216.8
ΔE_{oi}	−93.5	−104.0	−102.1
$\Delta E_{\text{int}}^{\neq}$	−50.2	−67.6	−64.5
$\Delta E_{\text{strain}}^{\neq}$	62.8	62.7	62.8
$\Delta E^{\neq}$	12.6	−4.9	−1.7
Fragment orbital overlaps $\langle \text{Pd}\vert\text{CH}_4\rangle$			
$\langle 4d\vert\text{LUMO}\rangle$	0.331	0.335	0.335
$\langle 5s\vert\text{HOMO}\rangle$	0.400	0.418	0.420
Fragment orbital populations (electrons)			
Pd: $4d$	9.34	9.26	9.29
$5s$	0.27	0.40	0.40
CH_4:HOMO	1.76	1.68	1.68
LUMO	0.39	0.41	0.41
Fragment orbital energies (eV)			
Pd: $4d$	−4.241	−4.186	−4.193
$5s$	−2.941	−3.504	−3.423
CH_4:HOMO	−7.234	−7.233	−7.232
LUMO	−2.111	−2.114	−2.113

[a]At BP86/TZ(2)P. NR=nonrelativistic, QR=quasirelativistic, ZORA=zeroth-order regular approximation (Sec. II B). Note that all analyses have been carried out using the NR geometry.

proach which also yields pronounced potential wells for reactant complexes that are consistent with relatively strongly bound, collisionally stabilized Pd-alkane reactant complexes observed in gas-phase experiments.

C. Analysis of activation energies and TS structures

To shed light on *how* the relativistic stabilization of transition states for oxidative insertion is brought about, we analyze the NR, QR and ZORA activation energies $\Delta E^{\neq}$ in terms of the activation strain $\Delta E_{\text{strain}}^{\neq}$ of and the TS-interaction $\Delta E_{\text{int}}^{\neq}$ between the deformed reactants in the activated complexes [see Eq. (6) and Sec. II C]. The results of these analyses are collected in Table III. Two trends can be recognized: (i) relativity increases the TS interaction $\Delta E_{\text{int}}^{\neq}$ (except for QR in **1c**, *vide infra*), and (ii) it lowers the activation strain $\Delta E_{\text{strain}}^{\neq}$ (except for ZORA in **3c**). Let's for example take the Pd+CH_4 reaction (**1**): if we go from NR to ZORA, the TS interaction increases from −50.2 to −55.1 kcal/mol and the activation strain decreases from 62.8 to 53.5 kcal/mol. Both the trend in TS interaction and activation strain can be understood quite straightforwardly as a consequence of the well-known relativistic effects[12] on the frontier d and s AOs of the Pd atom: going from NR to ZORA, the $4d$ HOMO is slightly *destabilized* (from −4.24 to −4.19 eV) and expanded, leading to a slight expansion of the overall Pd density, whereas the $5s$ LUMO is substantially *stabilized* (from −2.9 to −3.4 eV) and contracted (see Table III and Fig. 3). This leads to smaller energy gaps between the Pd $4d$ HOMO and the substrate LUMO (e.g., the $\sigma_{\text{C–H}}^{*}$ of CH_4) as well as between the Pd $5s$ LUMO and the substrate HOMO (e.g., the $\sigma_{\text{C–H}}$ of CH_4) and, therefore, to a stronger Pd-substrate bonding through increased π backdonation and σ donation, respectively (see Fig. 4 for relevant frontier orbital interactions).

The primary changes due to relativity in the Pd-substrate interaction are hidden to some extent by the structural changes they cause. Therefore, we have also analyzed the changes in TS interaction $\Delta E_{\text{int}}^{\neq}$ along NR, QR and ZORA using the optimum geometry of NR in all three cases. Table IV shows the results for the transition state of the Pd+CH_4 insertion (**1c**). Now, it becomes much more clear than in Table III that the main effect of relativity on the TS interaction is generated in the orbital interaction term ΔE_{oi}. If we go form NR to ZORA, the latter increases by 8.6 kcal/mol (from −93.5 to −102.1 kcal/mol) which accounts for nearly two-thirds of the relativistic strengthening of the TS interaction $\Delta E_{\text{int}}^{\neq}$. This correlates nicely with the reduced energy gaps between Pd and CH_4 frontier orbitals and it shows up in a decrease and increase of HOMO and LUMO populations, respectively (Table IV). Changes in the corresponding orbital overlaps are only marginal. Furthermore, the contributions of ΔV_{elst} and ΔE_{Pauli} to the trend in $\Delta E_{\text{int}}^{\neq}$, although not unimportant, are much smaller. Note that, in the analyses of Table IV, the trend in activation energy $\Delta E^{\neq}$ (e.g., the lowering by −14.3 kcal/mol if we go from NR to ZORA), is caused entirely by the trend in $\Delta E_{\text{int}}^{\neq}$ because the geometry is kept frozen (to the NR optimum), making the activation strain $\Delta E_{\text{strain}}^{\neq}$ essentially constant.

Next, the constraint of a frozen geometry is released as we go back to the analyses of Table III. One might at first expect that the stronger Pd-substrate interaction causes the Pd atom to be further inserted into the C–X bond in the TS. However, the opposite happens, i.e., relativity leads to a contraction of the C–X bond in a more eductlike TS. In fact, this is easily understood if we consider the schematic reaction profile in Fig. 5 which is based on quantitative analyses of all stationary points along the reaction coordinate (Tables III and IV only show the results for the TS). Here, the nonrelativistic energy ΔE of the reaction system is decomposed into the strain energy ΔE_{strain} of and interaction energy ΔE_{int} between the reactants (see Sec. II C). Along the reaction coordinate, ΔE_{strain} increases because the C–X bond of the substrate is stretched while the Pd-substrate interaction ΔE_{int} becomes more stabilizing due to the decreasing HOMO-LUMO gap of the substrate. The net result is the reaction profile of ΔE with the transition state indicated by an asterisk. Now, if relativistic effects are switched on, the curve of the strain energy ΔE_{strain} as a function of the reaction coordinate (or C–X bond stretching) is not much affected, but the Pd-substrate interaction increases in all points along the reaction coordinate. This strengthening, indicated by vertical arrows in Fig. 5, becomes larger as the reaction proceeds, simply because the inherent strength of Pd-substrate interaction also increases along this direction (*vide supra*). Thus, all stationary points on the relativistic PES, the dashed line in Fig. 5, are stabilized and the maximum shifts to the left, i.e., the TS becomes more reactantlike. This also accounts for the trend mentioned earlier (in Sec. III A) that the relativistic stabilization of stationary points relative to separate reactants increases in the order RC<TS<P. Finally, as can be seen in

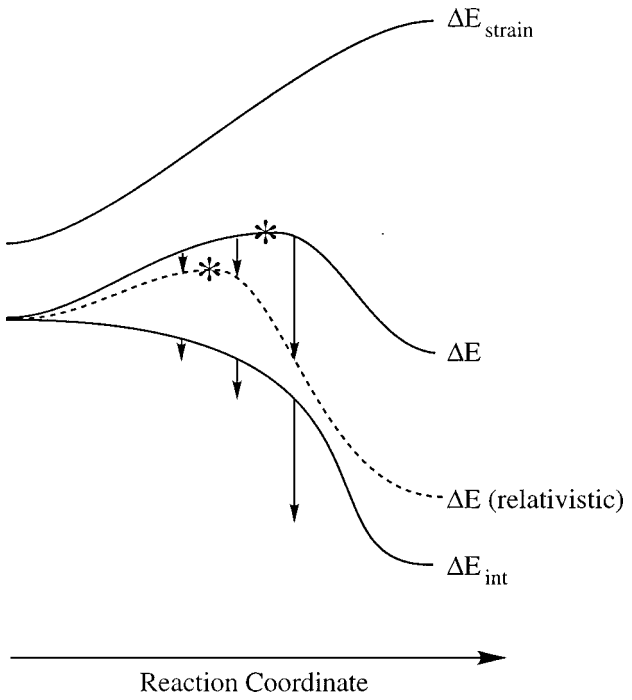

FIG. 5. Schematic representation of the nonrelativistic reaction profile provided by the energy ΔE of the reaction system and its decomposition into the strain energy ΔE_{strain} of and interaction energy ΔE_{int} [see Eq. (6)]. The relativistic strengthening of ΔE_{int} as well as the concomitant lowering of ΔE are indicated by vertical arrows (the resulting relativistic ΔE profile is shown as dashed line). Note that relativity stabilizes the TS (asterisk) and shifts it along the reaction coordinate toward the reactant complex.

Table III, the relativistic shift of the TS toward the reactant side is accompanied by a reduction in activation strain $\Delta E^{\neq}_{\text{strain}}$, in line with the smaller degree of C–X stretching (cf. ''reaction coordinate'' or scaled C–X distance in Table I).

IV. CONCLUSIONS

Relativistic effects are important for an accurate quantum chemical description of the oxidative insertion of the second-row transition metal palladium into C–H, C–C and C–Cl bonds, as follows from our nonlocal DFT study on the model systems CH_4, C_2H_6 and CH_3Cl, respectively, at BP86/TZ(2)P. The effect of relativity in both the quasirelativistic (QR) and, to a slightly lesser extent, in the ZORA approach is that stationary points along the reaction coordinate are stabilized with respect to reactants. This stabilization becomes stronger as the reaction proceeds, i.e., in the order reactant complex (RC)<transition state(TS)<product(P). Consequently, activation enthalpies are reduced by 6 (C–Cl) to 14 kcal/mol (C–H) and reaction enthalpies become more exothermic by 15 (C–Cl) to 20 kcal/mol (C–C). However, the relative order of barrier heights and reaction enthalpies is not affected. In all approaches, the activation barrier decreases in the order C–C>C–H>C–Cl and the reaction becomes more exothermic in the order C–H<C–C<C–Cl. Another relativistic effect is that all transition states become more eductlike.

The abovementioned effects can be understood in terms of the well-known relativistic destabilization of the Pd 4*d* HOMO and stabilization of the Pd 5*s* LUMO. These effects make the metal both a better electron donor and acceptor which leads to stronger donor–acceptor interactions between Pd and the substrate. The result is an additional stabilization of transition states and oxidative insertion products relative to the separate reactants.

Finally, the best agreement of our relativistic BP86/TZ(2)P results with *ab initio* PCI-80 benchmark values and gas-phase spectroscopic experiments is obtained using the zeroth-order regular approximation (ZORA). For activation energies, discrepancies of 8–9 kcal/mol remain which may be ascribed to the combined effect of an underestimation of barriers by DFT and the uncertainty of a few kcal/mol in the PCI-80 results.[7b,8a]

ACKNOWLEDGMENTS

One of the authors (A.D.) thanks the Fonds der Chemischen Industrie (FCI) for a doctoral stipendium. F.M.B. thanks the Deutsche Forschungsgemeinschaft (DFG) for a Habilitation fellowship and the FCI for financial support. Excellent service by the Hochschulrechenzentrum (HRZ) of the Philipps-Universität Marburg is gratefully acknowledged.

[1] (a) J. P. Collman, L. S. Hegedus, J. R. Norton, and R. G. Finke, *Principles and Applications of Organotransition Metal Chemistry* (University Science Books, Mill Valley, CA, 1987); (b) Ch. Elschenbroich and A. Salzer, *Organometallics. A Concise Introduction*, 2nd ed. (VCH, Weinheim, Germany, 1992); (c) C. Amatore and A. Jutand, Acc. Chem. Res. **33**, 314 (2000); (d) H. Yang, K. T. Kotz, M. C. Asplund, M. J. Wilknes, and C. B. Harris, *ibid.* **32**, 551 (1999); (e) A. Sen, *ibid.* **31**, 550 (1998).

[2] Experimental studies on reactions of metal complexes in the condensed phase: (a) T.-Y. Luh, M.-k. Leung, and K.-T. Wong, Chem. Rev. **100**, 3187 (2000); (b) R. Stürmer, Angew. Chem. **111**, 3509 (1999); (c) L.-B. Hau and M. Tanaka, Chem. Commun. (Cambridge) **5**, 395 (1999); (d) A. L. Casado and P. Espinet, Organometallics **17**, 954 (1998); (e) B. Kayser, C. Missling, J. Knizek, H. Noeth, and W. Beck, Eur. J. Inorg. Chem. **3**, 375 (1998); (f) M.-A. Guillevic, C. Rocaboy, A. M. Arif, I. T. Horvath, and J. A. Gladysz, Organometallics **17**, 707 (1998); (g) B. L. Edelbach, R. J. Lachicotte, and W. D. Jones, J. Am. Chem. Soc. **120**, 2843 (1998); (h) R. H. Crabtree, Chem. Rev. **95**, 987 (1995); (i) V. V. Grushin and H. Alper, *ibid.* **94**, 1047 (1994); (j) P. R. Ellis, J. M. Pearson, A. Haynes, H. Adams, N. A. Bailey, and P. M. Maitlis, Organometallics **13**, 3215 (1994); (k) M. W. Wright, T. L. Smalley, M. E. Welker, and A. L. Rheingold, J. Am. Chem. Soc. **116**, 6777 (1994); (l) T. Sakakaurka, T. Sodeyama, K. Sasaki, K. Wada, and M. Tanaka, *ibid.* **112**, 7221 (1990); (m) A. L. Casalnuovo, J. C. Calabrese, and D. Milstein, *ibid.* **110**, 6738 (1988); (n) A. H. Janowics and R. G. Bergman, *ibid.* **105**, 3929 (1983); (o) W. D. Jones and F. J. Feher, *ibid.* **104**, 4240 (1982); (p) C. E. Hickey and P. M. Maitlis, J. Chem. Soc. Chem. Commun. **1984** 1609; (q) D. Forster, in *Advances in Organometallic Chemistry*, edited by F. G. A. Stone and R. West (Academic, New York, 1979), Vol. 17, p. 255; (r) D. Forster, J. Am. Chem. Soc. **97**, 951 (1975).

[3] (a) K. Eller and H. Schwarz, Chem. Rev. **91**, 1121 (1991); (b) P. B. Armentrout and J. L. Beauchamp, Acc. Chem. Res. **22**, 315 (1989).

[4] Experimental studies on reactions of ionic metal atoms and complexes in the gas phase: (a) M. Brönstrup, D. Schröder, and H. Schwarz, Organometallics **18**, 1939 (1999); (b) M. Aschi, M. Brönstrup, M. Diefenbach, J. N. Harvey, D. Schröder, and H. Schwarz, Angew. Chem. **110**, 858 (1998); (c) B. S. Freiser, J. Mass Spectrom. **31**, 703 (1996); (d) P. A. M. van Koppen, P. R. Kemper, J. E. Bushnell, and M. T. Bowers, J. Am. Chem. Soc. **117**, 2098 (1995); (e) R. Wesendrup, D. Schröder, and H. Schwarz, Angew. Chem. **105**, 1232 (1994); (f) Y.-M. Chen, D. E. Clemmer, and P. B. Armentrout, J. Am. Chem. Soc. **116**, 7815 (1994); (g) K. J. van den Berg, S. Ingemann, N. M. M. Nibbering, and I. K. Gregor, Rapid Commun. Mass Spectrom. **7**, 769 (1993); (h) A. K. Chowdhury and C. L. Wilkins, J. Am. Chem. Soc. **109**, 5336 (1987); (i) D. A. Weil and C. L. Wilkins, *ibid.* **107**, 7316 (1985); (j) R. W. Jones and R. H. Staley, J. Phys. Chem. **86**, 1669 (1982); (k) R. W. Jones and R. H. Staley, J. Am. Chem. Soc. **102**, 3794 (1980).

[5] Combined experimental and theoretical studies on reactions of ionic metal atoms and complexes in the gas phase: (a) Q. Zhang, P. R. Kemper, S. K. Shin, and M. T. Bowers, Int. J. Mass. Spectrom. **204**, 281 (2001); (b) A. Sundermann, O. Uzan, D. Milstein, and J. M. L. Martin, J. Am. Chem. Soc. **122**, 7095 (2000); (c) S. S. Yi, E. L. Reichert, M. C. Holthausen, W. Koch, and J. C. Weisshaar, Chem. Eur. J. **6**, 2232 (2000); (d) M. Blomberg, S. S. Yi, R. J. Noll, and J. C. Weisshaar, J. Phys. Chem. A **103**, 7254 (1999); (e) M. Diefenbach, M. Brönstrup, M. Aschi, D. Schröder, and H. Schwarz, J. Am. Chem. Soc. **121**, 10614 (1999); (f) J. Schwarz, D. Schröder, H. Schwarz, C. Heinemann, and J. Hrusák, Helv. Chim. Acta **79**, 1110 (1996).

[6] Experimental studies on reactions of neutral metal atoms in the gas phase: (a) Y. Wen, M. Porembski, T. A. Ferrett, and J. C. Weisshaar, J. Phys. Chem. A **102**, 8362 (1998); (b) Y. Wen, A. Yethiraj, and J. C. Weisshaar, J. Chem. Phys. **106**, 5509 (1997); (c) J. J. Carroll, and J. C. Weisshaar, J. Phys. Chem. **100**, 12355 (1996); (d) G. V. Chertihin and L. Andrews, J. Am. Chem. Soc. **116**, 8322 (1994); (e) J. J. Carroll, K. L. Haug, and J. C. Weisshaar, *ibid.* **115**, 6962 (1993); (f) J. J. Carroll and J. C. Weisshaar, *ibid.* **115**, 800 (1993); (g) D. Ritter, J. J. Carroll, and J. C. Weisshaar, J. Phys. Chem. **96**, 10636 (1992); (h) S. A. Mitchell and P. A. Hackett, J. Chem. Phys. **93**, 7822 (1990); (i) D. Ritter and J. C. Weisshaar, J. Am. Chem. Soc. **112**, 6425 (1990); (j) P. Fayet, A. Kaldor, and D. M. Cox, J. Chem. Phys. **92**, 254 (1990).

[7] Combined experimental and theoretical studies on reactions of neutral metal atoms in the gas phase: (a) M. Porembski and J. C. Weisshaar, J. Phys. Chem. A **104**, 1524 (2000); (b) J. J. Carroll, K. L. Haug, J. C. Weisshaar, M. R. A. Blomberg, P. E. M. Siegbahn, and M. Svensson, J. Phys. Chem. **99**, 13955 (1995); (c) J. J. Carroll, J. C. Weisshaar, P. E. M. Siegbahn, A. M. C. Wittborn, and M. R. A. Blomberg, *ibid.* **99**, 14388 (1995); (d) S. Mitchell, M. A. Blitz, P. E. M. Siegbahn, and M. Svenson, J. Chem. Phys. **100**, 423 (1994); (e) J. C. Weisshaar, Acc. Chem. Res. **26**, 213 (1993).

[8] Theoretical studies on reactions of metal complexes: (a) A. Dedieu, Chem. Rev. **100**, 543 (2000); (b) M. Torrent, M. Solà, and G. Frenking, *ibid.* **100**, 439 (2000); (c) T. R. Griffin, D. B. Cook, A. Haynes, J. M. Pearson, D. Monti, and G. E. Morris, J. Am. Chem. Soc. **118**, 3029 (1996); (d) G. Aullón and S. Alvarez, Inorg. Chem. **35**, 3137 (1996); (e) T. Ziegler, Chem. Rev. **91**, 651 (1991); (f) N. Koga and K. Morokuma, *ibid.* **91**, 823 (1991); (g) F. M. Bickelhaupt, E. J. Baerends, and W. Ravenek, Inorg. Chem. **29**, 350 (1990); (h) O. V. Gritsenko, A. A. Bagatur'yants, I. I. Moiseev, and V. B. Kazanskii, Russ. Chem. Rev. **54**, 1151 (1985).

[9] See also, for example: (a) D. Lamprecht and G. J. Lamprecht, J. Comput. Chem. **21**, 692 (2000); (b) B. Minaev and H. Agren, Int. J. Quantum Chem. **72**, 581 (1999); (c) M.-D. Su and S.-Y. Chu, J. Am. Chem. Soc. **121**, 1045 (1999); (d) M.-D. Su and S.-Y. Chu, Inorg. Chem. **37**, 3400 (1998); (e) M.-D. Su and S.-Y. Chu, Chem. Phys. Lett. **282**, 25 (1998); (f) K. Albert, P. Gisdakis, and N. Rösch, Organometallics **17**, 1608 (1998); (g) S. Sakaki, B. Biswas, and M. Sugimoto, *ibid.* **17**, 1278 (1998); (h) G. S. Hill and R. J. Puddephatt, *ibid.* **17**, 1478 (1998); (i) S. Sakaki, M. Ogawa, and M. Kinoshita, J. Phys. Chem. **99**, 9933 (1995); (j) K. K. Irikura and W. A. Goddard III, J. Am. Chem. Soc. **116**, 8733 (1994); (k) J. K. Perry and W. A. Goddard III, *ibid.* **116**, 5013 (1994); (l) H. Sellers, J. Comput. Chem. **11**, 754 (1990); (m) M. Rosi, C. W. Bauschlicher, Jr., S. R. Langhoff, and H. Partridge, J. Phys. Chem. **94**, 8656 (1990); (n) T. Ziegler, V. Tschinke, L. Fan, and A. D. Becke, J. Am. Chem. Soc. **111**, 9177 (1989); (o) J. J. Low and W. A. Goddard III, *ibid.* **108**, 6115 (1986).

[10] (a) F. M. Bickelhaupt, J. Comput. Chem. **20**, 114 (1999); (b) F. M. Bickelhaupt, T. Ziegler, and P. von Ragué Schleyer, Organometallics **14**, 2288 (1995).

[11] Theoretical studies on reactions of neutral metal atoms: (a) A. M. C. Wittborn, M. Costas, M. R. A. Blomberg, and P. E. M. Siegbahn, J. Chem. Phys. **107**, 4318 (1997); (b) P. E. M. Siegbahn, J. Am. Chem. Soc. **116**, 7722 (1994); (c) P. E. M. Siegbahn, Organometallics **13**, 2833 (1994); (d) J. K. Perry, G. Ohanessian, and W. A. Goddard III, *ibid.* **13**, 1870 (1994); (e) M. R. A. Blomberg, P. E. M. Siegbahn, and M. Svensson, Inorg. Chem. **32**, 4218 (1993); (f) P. E. M. Siegbahn, M. R. A. Blomberg, and M. Svensson, J. Phys. Chem. **97**, 2564 (1993); (g) P. E. M. Siegbahn, M. R. A. Blomberg, and M. Svensson, J. Am. Chem. Soc. **115**, 1952 (1993); (h) P. E. M. Siegbahn, M. R. A. Blomberg, and M. Svensson, *ibid.* **115**, 4191 (1993); (i) P. E. M. Siegbahn and M. R. A. Blomberg, J. Am. Chem. Soc. **114**, 10548 (1992); (j) M. R. A. Blomberg, P. E. M. Siegbahn, and M. Svensson, *ibid.* **114**, 6095 (1992); (k) M. Svensson, M. R. A. Blomberg, and P. E. M. Siegbahn, *ibid.* **113**, 7076 (1991); (l) M. R. A. Blomberg, P. E. M. Siegbahn, U. Nagashima, and J. Wennerberg, *ibid.* **113**, 424 (1991); (m) E. A. Carter and W. A. Goddard III, J. Phys. Chem. **92**, 5679 (1988); (n) J. J. Low and W. A. Goddard III, Organometallics **5**, 609 (1986); (o) J. J. Low and W. A. Goddard III, J. Am. Chem. Soc. **106**, 8321 (1984).

[12] Relativistic effects: (a) R. E. Moss, *Advanced Molecular Quantum Mechanics* (Chapman and Hall, London, 1973); (b) P. Pyykkö, Chem. Rev. **88**, 563 (1988). See also: (c) F. Jensen, *Introduction to Computational Chemistry* (Wiley, Chichester, 1999).

[13] Density functional theory (DFT): (a) R. M. Dreizler and E. K. U. Gross, *Density Functional Theory. An Approach to the Quantum Many-Body Problem* (Springer, Berlin, 1990); (b) R. G. Parr and W. Yang, *Density-Functional Theory of Atoms and Molecules* (Oxford University Press, New York, 1989); (c) O. V. Gritsenko, B. Ensing, P. R. T. Schipper, and E. J. Baerends, J. Phys. Chem. A **104**, 8558 (2000).

[14] Kohn–Sham MO model in DFT: (a) F. M. Bickelhaupt and E. J. Baerends, in *Reviews in Computational Chemistry*, Vol. 15, edited by K. B. Lipkowitz and D. B. Boyd. (Wiley-VCH, New York, 2000), pp. 1–86; (b) E. J. Baerends and O. V. Gritsenko, J. Phys. Chem. A **101**, 5383 (1997).

[15] A. Diefenbach and F. M. Bickelhaupt (unpublished).

[16] Amsterdam Density Functional (ADF) program: (a) C. Fonseca Guerra, O. Visser, J. G. Snijders, G. te Velde, and E. J. Baerends, in *Methods and Techniques for Computational Chemistry*, edited by E. Clementi, and G. Corongiu (STEF, Cagliari, 1995), pp. 305–395; (b) G. te Velde, F. M. Bickelhaupt, E. J. Baerends, S. J. A. van Gisbergen, C. Fonseca Guerra, J. G. Snijders, and T. Ziegler, J. Comput. Chem. **22**, 931 (2001); (c) E. J. Baerends, D. E. Ellis, and P. Ros, Chem. Phys. **2**, 41 (1973); (d) C. Fonseca Guerra, J. G. Snijders, G. te Velde, and E. J. Baerends, Theor. Chem. Acc. **99**, 391 (1998); (e) P. M. Boerrigter, G. te Velde, and E. J. Baerends, Int. J. Quantum Chem. **33**, 87 (1988); (f) G. te Velde and E. J. Baerends, J. Comput. Phys. **99**, 84 (1992); (g) J. G. Snijders, E. J. Baerends, and P. Vernooijs, At. Data Nucl. Data Tables **26**, 483 (1982); (h) J. Krijn and E. J. Baerends, *Fit-Functions in the HFS-Method*, internal report in Dutch, Vrije Universiteit, Amsterdam, 1984; (i) A. D. Becke, J. Chem. Phys. **84**, 4524 (1986); (j) A. Becke, Phys. Rev. A **38**, 3098 (1988); (k) S. H. Vosko, L. Wilk, and M. Nusair, Can. J. Phys. **58**, 1200 (1980); (l) J. P. Perdew, Phys. Rev. B **33**, 8822 (1986), erratum: *ibid.* **34**, 7406 (1986); (m) L. Fan and T. Ziegler, J. Chem. Phys. **94**, 6057 (1991); (n) L. Versluis and T. Ziegler, *ibid.* **88**, 322 (1988); (o) L. Fan and T. Ziegler, *ibid.* **92**, 3645 (1990); (p) L. Fan, L. Versluis, T. Ziegler, E. J. Baerends, and W. Ravenek, Int. J. Quantum Chem., Quantum Chem. Symp. **S22**, 173 (1988).

[17] P. W. Atkins, *Physical Chemistry* (Oxford University Press, Oxford, 1998).

[18] Quasirelativistic approach: (a) P. Boerrigter, Thesis, Vrije Universiteit, Amsterdam, 1987; (b) P. Boerrigter, E. J. Baerends, and J. G. Snijders, Chem. Phys. **122**, 357 (1988); (c) T. Ziegler, V. Tschinke, E. J. Baerends, J. G. Snijders, and W. Ravenek, J. Phys. Chem. **93**, 3050 (1989). (d) See also, for example: T. Ziegler, J. G. Snijders, and E. J. Baerends, in *The Challenge of d and f Electrons*, edited by D. R. Salahub and M. C. Zerner, ACS Symposium Series 395, American Chemical Society, 1989, p. 322; (e) H. Jacobson, G. Schreckenbach, and T. Ziegler, J. Phys. Chem. **98**, 11406 (1994); (f) J. Li, G. Schreckenbach, and T. Ziegler, Inorg. Chem. **34**, 3245 (1995).

[19] Pauli Hamiltonian and first-order perturbation approach: (a) J. G. Snijders and E. J. Baerends, Mol. Phys. **36**, 1789 (1978); (b) J. G. Snijders, E. J. Baerends, and P. Ros, *ibid.* **38**, 1909 (1979); (c) R. D. Cowan and D. C. Griffin, J. Opt. Soc. Am. **66**, 1010 (1976); (d) L. L. Foldy and S. A. Wouthuysen, Phys. Rev. **78**, 29 (1950). See also Ref. 12a.

[20] ZORA approach: (a) C. Chang, M. Pelissier, and P. Durand, Phys. Scr. **34**, 394 (1986); (b) E. van Lenthe, E. J. Baerends, and J. G. Snijders, J. Chem. Phys. **99**, 4597 (1993); (c) E. van Lenthe, J. G. Snijders, and E. J. Baerends, J. Chem. Phys. **105**, 6505 (1996); (d) E. van Lenthe, *Thesis*, Vrije Universiteit, Amsterdam, 1996; (e) E. van Lenthe, R. van Leeuwen, E. J. Baerends, and J. G. Snijders, Int. J. Quantum Chem. **57**, 281 (1996).

[21] Bond energy decomposition: (a) T. Ziegler and A. Rauk, Inorg. Chem. **18**, 1558 (1979); *ibid.* **18**, 1755 (1979); *ibid.* **46**, 1 (1977); (d) F. M. Bickelhaupt, N. M. M. Nibbering, E. M. van Wezenbeek, and E. J. Baerends, J. Phys. Chem. **96**, 4864 (1992).

[22] G. S. Hammond, J. Am. Chem. Soc. **77**, 334 (1955).

[23] See, for example: (a) N. M. M. Nibbering, Acc. Chem. Res. **23**, 279 (1990); (b) J. M. Riveros, S. M. José, and K. Takashima, Adv. Phys. Org. Chem. **21**, 197 (1985); (c) Ref. 10a. See also: (d) F. M. Bickelhaupt, N. M. M. Nibbering, E. J. Baerends, and T. Ziegler, J. Am. Chem. Soc. **115**, 9160 (1993).